

Adaptive cancellation of floor vibrations in standing ballistocardiogram measurements using a seismic sensor as a noise reference

Omer T. Inan*, *Student Member, IEEE*, Mozziyar Etemadi, *Student Member, IEEE*, Bernard Widrow, *Life Fellow, IEEE*, and Gregory T. A. Kovacs, *Fellow, IEEE*

Abstract—An adaptive noise canceller was used to reduce the effect of floor vibrations on ballistocardiogram (BCG) measurements from a modified electronic bathroom scale. A seismic sensor was placed next to the scale on the floor and used as the noise reference input to the noise canceller. BCG recordings were acquired from a healthy subject while another person stomped around the scale, causing increased floor vibrations. The noise canceller substantially eliminated the artifacts in the BCG signal due to these vibrations without distorting the morphology of the measured BCG. Additionally, recordings were obtained from another subject standing inside of a parked bus while the engine was running. The artifacts due to the vibrations of the engine, and the other vehicles driving by the bus on the road, were also effectively eliminated by the noise canceller. The system with automatic floor vibration cancellation could be used to increase BCG measurement robustness in home monitoring applications. Additionally, the noise cancellation approach may enable BCG recording in ambulances—or other transport vehicles—where non-invasive hemodynamic monitoring may otherwise not be feasible.

Index Terms—Physiological monitoring, cardiovascular disease, ballistocardiogram, adaptive noise cancellation.

I. INTRODUCTION

BALLISTOCARDIOGRAPHY is a non-invasive technique for assessing myocardial strength and vascular health [1], [2]. The ballistocardiogram (BCG) signal results from the reaction forces on the body caused by cardiac ejection of blood through the vasculature. Many systems have been described in the literature for BCG measurement, including those using tables [2], [3], beds [4], electromagnets [5], chairs [6], and weighing scales [7]–[9]. The systems using weighing scales have several practical advantages over the alternatives, in terms of compactness, ease of use, and long-term reliability.

Copyright (c) 2009 IEEE. Personal use of this material is permitted. However, permission to use this material for other purposes must be obtained from the IEEE by sending an email to pubs-permissions@ieee.org.

Manuscript received December 8, 2008; revised January 22, 2009. O. T. Inan was supported by the G. J. Lieberman Fellowship (Stanford University) and M. Etemadi was supported by the Electrical Engineering Fellowship (Stanford University). Asterisk (*) indicates corresponding author.

*O. T. Inan is with the Department of Electrical Engineering, Stanford University, Stanford, CA, 94305 USA (e-mail: omeri@stanford.edu, Phone: (650) 723-5646).

M. Etemadi and B. Widrow are with the Department of Electrical Engineering, Stanford University, Stanford, CA, 94305 USA (e-mail: metemadi@stanford.edu, widrow@stanford.edu).

G. T. A. Kovacs is with the Department of Electrical Engineering and the School of Medicine, Stanford University, Stanford, CA, 94305 USA (e-mail: kovacs@cis.stanford.edu).

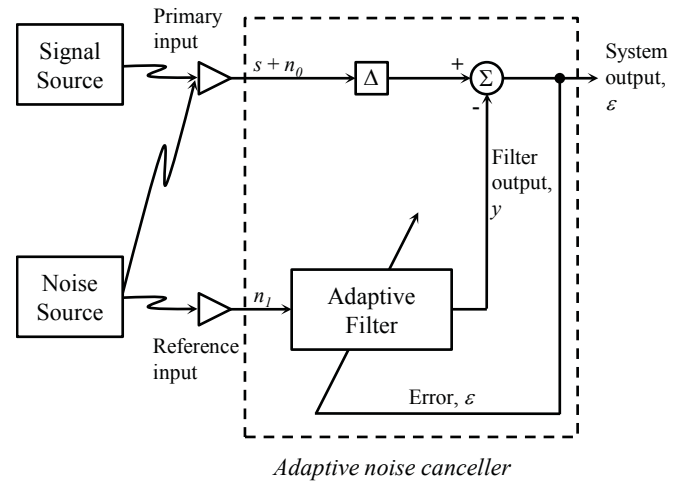


Fig. 1. Adaptive noise cancellation concept, adapted from [10].

As a result, these systems are well suited for home monitoring applications.

However, one disadvantage of using a weighing scale for BCG measurement is the increased susceptibility to motion artifacts and floor vibrations. Motion artifacts are pronounced in these measurements since the user stands on the device rather than sitting or lying prone. Floor vibrations affect the signal since the measurement axis is parallel to the primary direction of the vibrations. To increase measurement robustness, a second sensor, indicative of the motion or floor vibration, can be used as a noise reference for artifact detection and cancellation.

For motion artifact detection, a recent study proposed the electromyogram (EMG) signal taken from the feet of the subject as the noise reference [7]. For floor vibration detection, this paper proposes a seismic sensor, placed in close proximity to the scale, as the noise reference. An adaptive algorithm is then used to filter the output of this sensor and cancel the vibrations from the measured BCG.

II. THEORY AND SYSTEM DESIGN

A. Theory of adaptive noise cancellation

The basic adaptive noise cancellation architecture is shown in Fig. 1, after Widrow, *et al.* [10]. The noise canceller has two inputs, the primary and the reference inputs, and one output, the system output. One sensor at the primary input receives

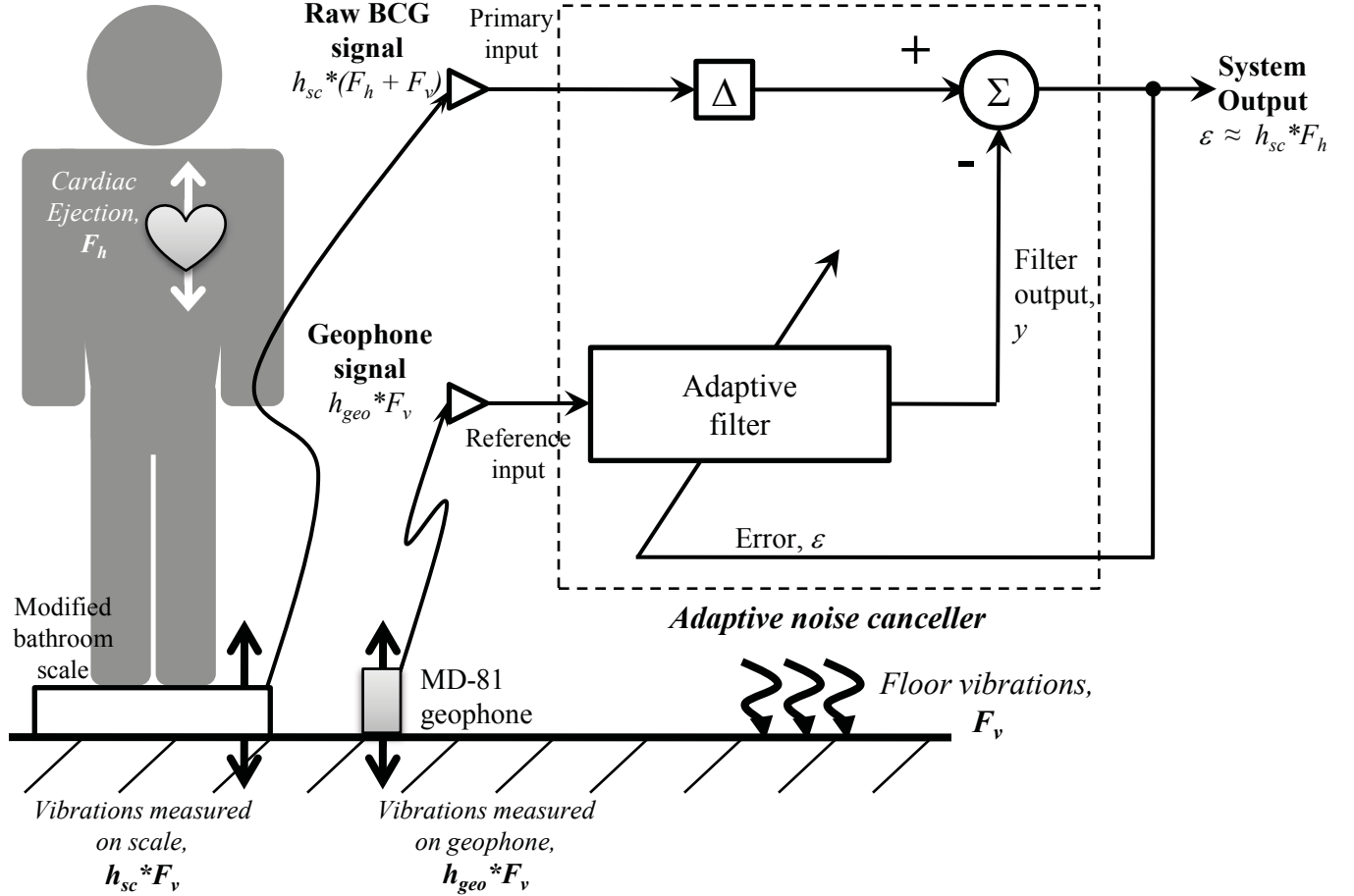


Fig. 2. Measurement setup: The subject stands on the scale while the force of cardiac ejection, F_h , and floor vibrations, F_v , are sensed by the scale. Simultaneously, the floor vibrations are sensed by the geophone. The scale and geophone signals are inputted to an adaptive noise canceller, and the system output is the best least-squares estimate of the cardiac signal.

some signal of interest, s , combined with an uncorrelated noise, n_0 . A second sensor at the reference input receives a noise, n_1 , which is correlated to n_0 by some unknown transfer function. The noise at the reference input is then filtered adaptively to match the noise component of the primary input, as shown below. For a more detailed treatment of the theory of adaptive noise cancellation, the reader is referred to the literature [10], [11].

Assume that s , n_0 , n_1 , and y are statistically stationary and have zero means; s is uncorrelated with n_0 and n_1 ; and n_0 is correlated with n_1 . Using an adaptive algorithm, as discussed below, the filter will adjust its weights, at each iteration, to minimize the mean-square error. The error signal, ϵ , is also the system output, and can be written as:

$$\epsilon = s + n_0 - y \quad (1)$$

The square of the error is then:

$$\epsilon^2 = s^2 + (n_0 - y)^2 + 2s(n_0 - y) \quad (2)$$

The expected value of both sides of this equation can then be computed to find the mean-square error:

$$\begin{aligned} E[\epsilon^2] &= E[s^2] + E[(n_0 - y)^2] + 2E[s(n_0 - y)] \\ &= E[s^2] + E[(n_0 - y)^2] \end{aligned} \quad (3)$$

The $E[s(n_0 - y)]$ term goes to zero since s is uncorrelated with n_0 and n_1 , and y is a filtered version of n_1 . Since the filter cannot affect the signal power, $E[s^2]$, the minimum mean-square error will be achieved when $E[(n_0 - y)^2]$ is minimized. The filter output, y , is thus the best least-squares estimate of the primary noise, n_0 . Finally, when $E[(n_0 - y)^2]$ is minimized, $E[(\epsilon - s)^2]$ is also minimized, since

$$(\epsilon - s) = (n_0 - y) \quad (4)$$

As a result, the system output, ϵ , is the best least-squares estimate of the primary signal.

In this paper, the LMS algorithm [11] was used to update the weights of the adaptive filter:

$$\mathbf{W}_{k+1} = \mathbf{W}_k + 2\mu\epsilon_k\mathbf{X}_k \quad (5)$$

where \mathbf{W}_k is a $1 \times L$ vector of weights at a given iteration, k ; μ is the learning rate of the filter that controls speed and stability of the adaptation; ϵ is the error signal fed back to the filter; \mathbf{X}_k is the vector of input samples to the filter; and \mathbf{W}_{k+1} is the vector of weights to be used in the next iteration. With this algorithm, the misadjustment—or the normalized excess mean-square error—will be given by:

$$M = \mu \text{tr}[\mathbf{R}] \quad (6)$$

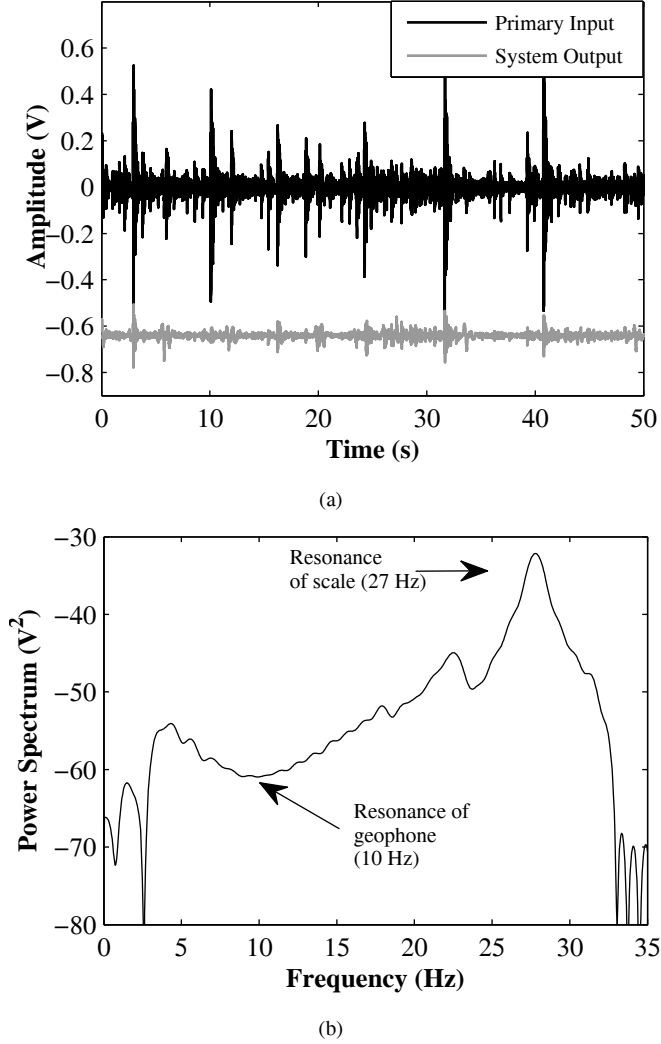


Fig. 3. (a) Primary input (weighing scale output) and filtered output using the optimum parameters for the adaptive filter ($L = 250$ taps, $M = 1\%$, $\Delta = 62$ samples). The noise reduction was 12dB. (b) Frequency response of the adaptive filter after convergence. The response dips at the geophone resonance (10Hz) and peaks at scale resonance (27Hz with $m = 40$ kg).

where M is the misadjustment, and $\text{tr}[\mathbf{R}]$ is the trace of the autocorrelation matrix, \mathbf{R} , for the input vector, \mathbf{X} . The general expression for the time constant of the learning curve, τ_{MSE} , assuming equal eigenvalues of the \mathbf{R} matrix, is given by:

$$\tau_{\text{MSE}} = \frac{L+1}{4M} \quad (7)$$

In many cases, this is also a good approximation when the eigenvalues of \mathbf{R} are unequal [11]. The process used for selecting the optimum parameters for the filter is described below, in Section II-C.

B. Measurement setup and electronics

Fig. 2 shows the measurement setup. During the BCG measurement, the subject stands on a commercial bathroom scale with modified electronics. With each heartbeat, a contractile force, F_h , is exerted by the heart on the blood and an equal but opposite force is experienced by the body. This causes vertical body motion synchronized with the beating heart.

The BCG signal is sensed by the strain gauges in the scale through some transfer function, h_{sc} , and amplified using an analog circuit with a gain of 11,000 and a bandwidth from 0.1–24Hz. The scale has four strain gauges that are connected in a Wheatstone bridge, excited by a $\pm 9\text{V}$ DC voltage. A commercial instrumentation amplifier (LT1167, Linear Technology, Milpitas, CA) boosts the differential voltage across the bridge by a factor of 100 and converts it to a single-ended signal. An integrator in the feedback loop of the LT1167 output stage is used to servo the low frequency components of the signal to zero—this has an overall high-pass filtering effect with a 3dB cutoff frequency of 0.1Hz. This stage is then AC-coupled to a Sallen-and-Key low-pass filter with a 3dB cutoff frequency of 24Hz. The final stage is a non-inverting amplifier with a gain of 111.

In addition to the forces due to cardiac ejection, forces due to floor vibrations, F_v , are also coupled to the scale through this same transfer function, h_{sc} . These vibrations can corrupt the signal quality of the BCG, reducing the robustness of the recording. To attenuate the artifacts caused by these vibrations in the BCG signal, an adaptive noise canceller was implemented with a seismic sensor (MD-81 Geophone, Geosource Inc., Houston, TX) placed on the floor next to the scale as the noise reference. This geophone sensed the same floor vibrations, F_v , through a different transfer function, h_{geo} .

The circuit used for amplifying and filtering the geophone signal was a simple non-inverting amplifier stage AC-coupled to a Sallen-and-Key low-pass filter—the overall gain was 101 and the bandwidth was 0.1–24Hz. Both the BCG and geophone signals were sampled at 1kHz using a data acquisition card (6024E, National Instruments, Austin, TX) and stored on a laptop computer using software (Matlab, Version 2007b, The Mathworks, Natick, MA). The signals were downsampled to 200Hz prior to the filtering operations.

If the transfer function of the scale, h_{sc} , and of the geophone, h_{geo} , were time invariant, and could be measured prior to the BCG recording, the noise could be cancelled using a straightforward approach: the geophone signal could be passed through an optimum filter composed of the inverse of the geophone transfer function cascaded with the transfer function of the scale. The resulting output would, in theory, be exactly equal to $h_{sc} * F_v$, where $*$ is the convolution operator. Unfortunately, the transfer function of the scale, h_{sc} , can vary significantly based on the properties of the scale and the mass and other physical characteristics of the subject, and can be quite different from person to person. As a result, an adaptive noise cancelling architecture was implemented, with the raw BCG signal as the primary input and the geophone signal as the reference input. With this approach, the adaptive filter automatically, and continually, adjusted its impulse response to best map the geophone signal to the floor vibrations component of the measured BCG to achieve cancellation of these vibrations.

C. System performance: Loading the scale with iron weights

The setup shown in Fig. 2, where the person on the scale was replaced by iron weights, was used to tune the parameters

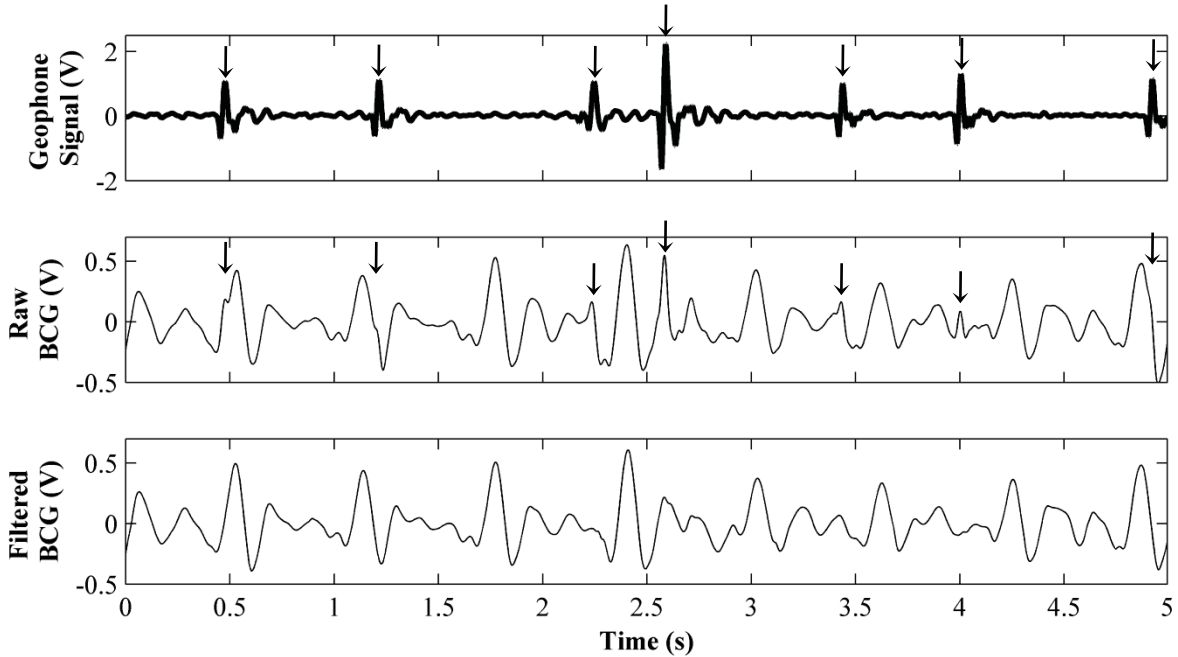


Fig. 4. Top trace: geophone signal output of amplifier. Middle trace: measured BCG signal with vibration-induced artifacts highlighted by black arrows. Bottom trace: filtered BCG output of noise canceller. The vibration artifacts are substantially eliminated in the filtered signal, without distorting the morphology of the BCG.

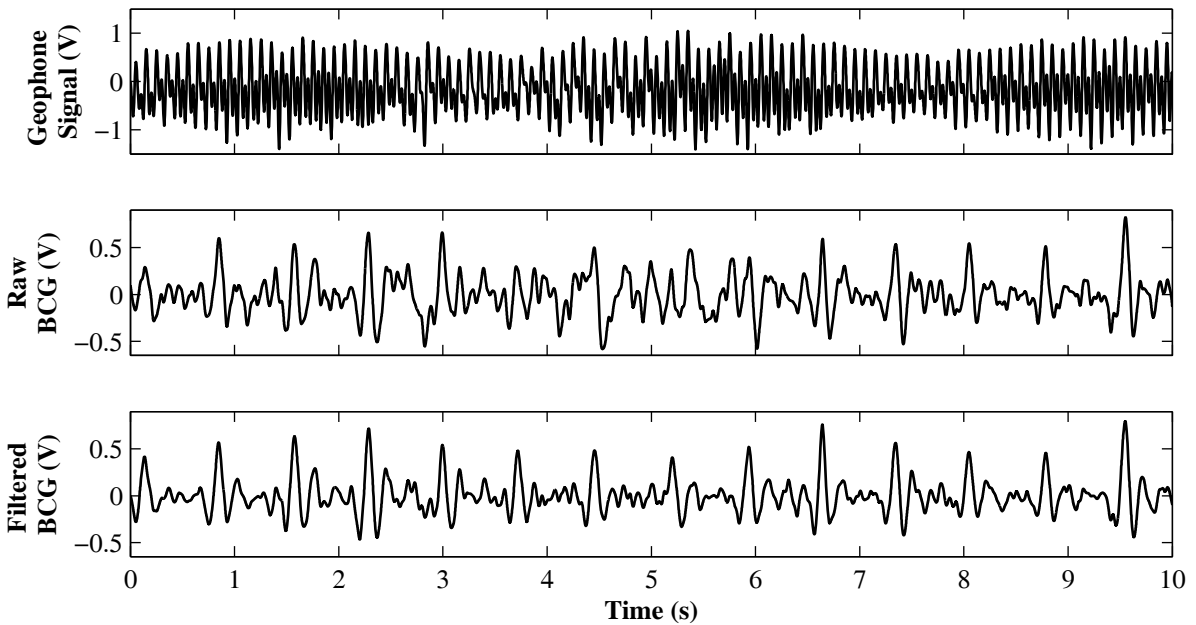


Fig. 5. BCG recordings taken from a subject standing in a parked bus. Top trace: geophone output of the amplifier. Middle trace: raw BCG signal output of amplifier with significant vibration-induced artifacts. These artifacts were caused by the engine of the bus as well as other vehicles driving on the road. Bottom trace: filtered BCG output of the noise canceller. The artifacts due to vibrations have been significantly eliminated from the recording.

of the adaptive filter: length (L), misadjustment (M), and delay (Δ) in the desired response path. The delay in the desired response is necessary in practice to allow the adaptive filter response to approximate a two-sided impulse response [11]. The iron weights on the scale were of mass, $m = 40\text{kg}$, and the scale output and geophone output were recorded while

a person stomped around the scale to create significant floor vibrations. With this setup, the BCG signal source was set to zero since no subject was standing on the scale. The adaptive filter weights were initialized at zero and the parameters were varied to maximize the noise reduction, ΔN , defined as the ratio of the variances of the scale output and the system output,

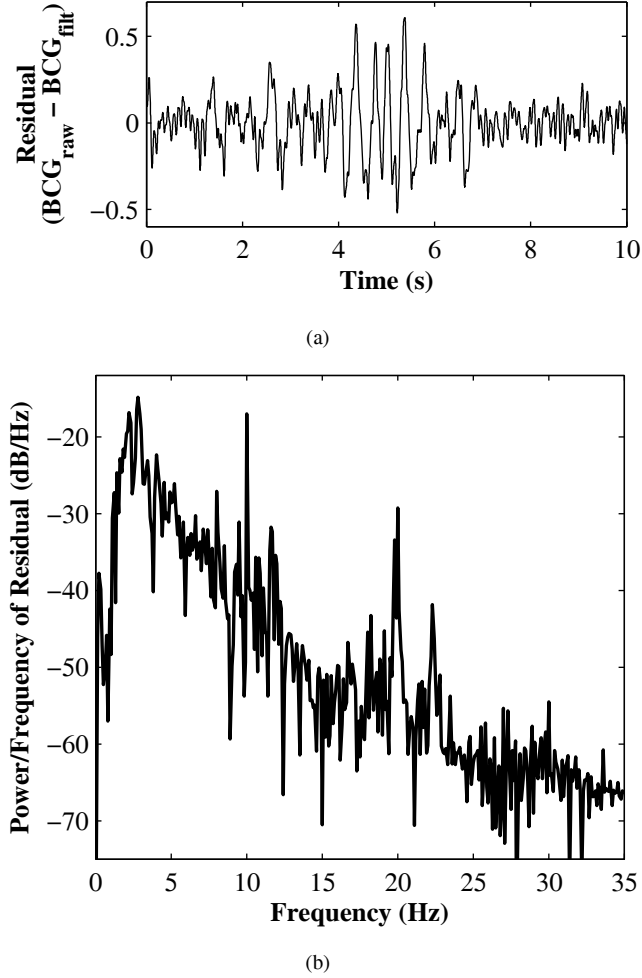


Fig. 6. (a) Residual computed from the raw and filtered BCG signals shown in Fig. 5. (b) Power spectral density estimate of this residual computed using the fast Fourier transform (FFT) of the autocorrelation sequence. The frequency content of the noise has higher frequency peaks which could be reduced by linear filtering, but also contains significant low frequency content that overlaps with the bandwidth of the BCG (1–10Hz). The adaptive noise canceller effectively eliminates these artifacts from the signal.

expressed in dB:

$$\Delta N = 10 \log_{10} \left(\frac{\text{var}(h_{sc} * F_V)}{\text{var}(\epsilon)} \right) \quad (8)$$

A maximum noise reduction of 12dB was achieved with a filter length, L , of 250 taps, a misadjustment, M , of 1%, and a desired response delay, Δ , of 62 samples ($L/4$). Using equation 7, these parameters correspond to a convergence time constant, τ_{MSE} , of 6,275 samples, or approximately 31 seconds. For real-time implementations, this convergence time constant could be reduced by increasing the misadjustment with a slight decrease in noise reduction. The recorded signal and the system output of the canceller using these parameters are shown in Fig. 3(a). Fig. 3(b) shows the frequency response of the adaptive filter after convergence. Interestingly, the response of this filter has a dip at the resonant frequency of the geophone (10Hz) and a peak at the resonant frequency of the scale (27Hz), calculated based on the spring constant of the scale measured in a previous study ($1.16N/\mu m$) [12]. This frequency response

is consistent with the expected response of the optimum filter discussed above: the adaptive filter response is the inverse transfer function of the geophone cascaded with the transfer function of the scale. With loads on the scale other than 40kg, the same results are obtained by the noise canceller, as soon as the adaptive filter converges. With a filter length of 250 taps and a delay of 62 samples, a 1% misadjustment was achieved with a 31 second convergence time constant.

III. RESULTS AND DISCUSSION

The BCG and geophone signals were recorded from a healthy subject standing on the scale while another person stomped around the scale to cause significant floor vibrations. The subject on the scale was 1.65m in height, 54kg in weight, and 22 years of age. The adaptive filter parameters determined in Section II-C were used, and a filtered BCG signal was obtained by using the noise canceller. The results are shown in Fig. 4. The top trace is the geophone signal from the amplifier. The middle trace is the measured BCG waveform, with vibration artifacts highlighted by black arrows. The bottom trace is the filtered BCG output of the adaptive noise canceller, where these artifacts have been removed by the adaptive filter.

In some instances, the artifacts appear as distortions in the morphology of the signal, such as the first artifact at the time $t = 0.5s$ into the recording. These types of artifacts could lead to a misinterpretation of the signal, resulting in a misdiagnosis of the cardiovascular health of the subject. In other instances, the artifacts appear as extra peaks in the signal, such as the artifact at the time $t = 2.6s$ into the recording. These types of artifacts could lead to errors in heart beat and arrhythmia detection.

To ensure that the output of the noise canceller did not distort the average signal morphology of the BCG, the ensemble average of both the raw signal and the filtered signal were computed and compared. A residual was computed by subtracting the average filtered signal from the average raw signal. The variance of this residual was 0.09% of the variance of the original signal average, demonstrating that the signal morphology was adequately preserved in the filtering.

The signals were acquired from another healthy subject while standing inside of a bus. The subject was 1.75m in height, 63.6kg in weight, and 25 years of age. When the bus was in motion, the BCG and geophone amplifier outputs railed, preventing the use of adaptive noise cancelling for removing the vibrations. However, when the bus was parked, the signals were acquired successfully without railing the amplifier. In these recordings, the vibrations due to the engine and the other vehicles driving on the road corrupted the signal quality of the BCG significantly. The noise cancellation algorithm was used to eliminate the vibrations from the measured BCG. The results are shown in Fig. 5.

The top trace shows the geophone amplifier output. The middle trace shows the measured BCG waveform. Many of the BCG beats are completely obscured by the vibration noise from the bus. The bottom trace shows the filtered BCG waveform, where the vibration artifacts have been significantly eliminated.

The residual of the raw and filtered BCG signals of Fig. 5 was computed to analyze the nature of the vibration noise, and is shown in Fig. 6(a). Fig. 6(b) shows the power spectral density (PSD) estimate for this residual. The PSD was estimated by taking the fast Fourier transform (FFT) of the autocorrelation sequence of the residual. While some of the noise power appears to be outside of the useful bandwidth of the BCG (1–10Hz), a majority of the power overlaps in frequency with the BCG and, thus, could not be removed by simple linear filtering operations; all components were, however, removed quite effectively by the adaptive noise cancellation algorithm. Nevertheless, future work should focus on developing other algorithms for cancelling these vibration artifacts from the BCG as well, including possibly using parametric spectral estimation techniques for determining the optimum filter described in Section II-B.

IV. CONCLUSIONS

The use of a seismic sensor as a noise reference to eliminate floor vibrations from standing BCG measurements was demonstrated. As a result, high fidelity BCG recording is possible in nearly all settings, including ambulances and other transport vehicles, provided that the vibrations are not so significant as to rail the electronics or cause a distorted version of the BCG forces to be coupled to the scale.

While in this paper a geophone was used as the seismic sensor, other sensors such as accelerometers could also be used with the same approach. Additionally, similar methods could be applied to other BCG measurement modalities such as chair- or bed-based systems, where the seismic sensor could be implanted into the structure of the measurement system itself. These approaches would increase the robustness of BCG measurements, allowing the BCG to be a useful tool for cardiovascular monitoring at home.

ACKNOWLEDGMENT

The authors thank Richard Wiard and Dr. Laurent Giovangrandi for their useful technical discussions and feedback, and Michael Chen for his time in supporting the project.

REFERENCES

- [1] H. R. Brown, V. de Lalla, M. A. Epstein, and M. J. Hoffman, *Clinical ballistocardiography*, New York: Macmillan, 1952.
- [2] I. Starr, A. J. Rawson, H. A. Schroeder, and N. R. Joseph, "Studies on the Estimation of Cardiac Output in Man, and of Abnormalities in Cardiac Function, From the Heart's Recoil and the Blood's Impacts; The Ballistocardiogram," *The Am. J. of Physiol.*, vol. 127, no. 1, 1939.
- [3] J. L. Nickerson, and H. J. Curtis, "The Design of the Ballistocardiograph," *The Am. J. Physiol.*, vol. 142, no. 1, pp. 1-11, 1944.
- [4] J. Alihanka, K. Vaahtoranta, and I. Saarikivi, "A new method for long-term monitoring of the ballistocardiogram, heart rate, and respiration," *The Am. J. of Phys.*, vol. 240, no. 5, pp. R384, 1981.
- [5] W. Dock, and F. Taubman, "Some technics for recording the ballistocardiogram directly from the body," *Am. J. Med.*, vol. 7, no. 6, pp. 751-5, illust, Dec, 1949.
- [6] T. Koivostoinen, S. Junnila, A. Varri et al., "A new method for measuring the ballistocardiogram using EMFi sensors in a normal chair." pp. 2026-2029.
- [7] O. T. Inan, M. Etemadi, R. M. Wiard, L. Giovangrandi, and G. T. A. Kovacs, "Evaluating the Foot Electromyogram Signal as a Noise Reference for a Bathroom Scale Ballistocardiogram Recorder," *IEEE CBMS*, Jyvaskyla, Finland, 2008.
- [8] O. T. Inan, M. Etemadi, R. M. Wiard, G. T. A. Kovacs, and L. Giovangrandi, "Non-invasive measurement of Valsalva-induced hemodynamic changes on a bathroom scale Ballistocardiograph," *IEEE EMBC*, Vancouver, Canada, 2008.
- [9] J. Williams, "Bridge Circuits—Marrying Gain and Balance," *Linear Technology Application Note*, vol. AN43, pp. 1-46, 1990.
- [10] B. Widrow, J. R. Glover, Jr., J. M. McCool et al., "Adaptive noise cancelling: Principles and applications," *Proc. of the IEEE*, vol. 63, no. 12, pp. 1692-1716, 1975.
- [11] B. Widrow, and S. D. Stearns, *Adaptive signal processing*, Prentice-Hall, Inc., 1985.
- [12] O. T. Inan, M. Etemadi, R. M. Wiard, L. Giovangrandi, and G. T. A. Kovacs, "Robust Ballistocardiogram Acquisition for Home Monitoring," *Phys. Meas.*, vol. 30, no. 2, pp. 169-185, 2009.



Omer T. Inan (S'06) received the B.S. and M.S. degrees in electrical engineering from Stanford University, Stanford, CA, in 2004 and 2005, respectively. He is currently pursuing the Ph.D. degree in electrical engineering at Stanford University.

He joined ALZA Corporation (A Johnson & Johnson Co.) in 2006 as an engineering intern in the Drug Device Research and Development (DDR) Group. With DDRD, he designed circuits for an iontophoretic drug delivery device, and researched options for innovative drug delivery systems. In 2007, he joined Countryman Associates Inc. as a Senior Engineer, working on high-end professional audio circuits and systems. His current research interests at Stanford University include circuit and system design for biomedical instrumentation, space biology applications, and home diagnostics, as well as novel signal processing algorithms for biosignal classification and noise reduction.

Mr. Inan received the Gerald J. Lieberman Fellowship (Stanford University) in 2008 for outstanding teaching and scholarship. He is a Three-Time NCAA All-American in the discus throw, and a former co-captain of the Stanford University Track and Field Team.



Moziyar Etemadi (S'07) received the B.S. degree in electrical engineering from Stanford University in 2008. He is currently pursuing the M.S. degree in electrical engineering at Stanford University, and is in the process of deciding where he will begin his M.D./Ph.D. training in the fall of 2009. His current research interests are in the areas of translational biomedical engineering, biomedical signal processing, and biomedical instrumentation for home monitoring.

In 2008, Mr. Etemadi received the Frederick E. Terman Award for Scholastic Achievement in Engineering. Mr. Etemadi also received the Electrical Engineering Fellowship (Stanford University), providing full support for his graduate studies.



Bernard Widrow (M'58-SM'75-F'76-LF'95) received the S.B., S.M., and Sc.D. degrees in Electrical Engineering from the Massachusetts Institute of Technology in 1951, 1953, and 1956, respectively. He joined the MIT faculty and taught there from 1956 to 1959. In 1959, he joined the faculty of Stanford University, where he is currently Professor of Electrical Engineering.

He began research on adaptive filters, learning processes, and artificial neural models in 1957. Together with M.E. Hoff, Jr., his first doctoral student at Stanford, he invented the LMS algorithm in the autumn of 1959. Today, this is the most widely used learning algorithm, used in every MODEM in the world. He has continued working on adaptive signal processing, adaptive controls, and neural networks since that time.

Dr. Widrow is a Life Fellow of the IEEE and a Fellow of AAAS. He received the IEEE Centennial Medal in 1984, the IEEE Alexander Graham Bell Medal in 1986, the IEEE Signal Processing Society Medal in 1986, the IEEE Neural Networks Pioneer Medal in 1991, the IEEE Millennium Medal in 2000, and the Benjamin Franklin Medal for Engineering from the Franklin Institute of Philadelphia in 2001. He was inducted into the National Academy of Engineering in 1995 and into the Silicon Valley Engineering Council Hall of Fame in 1999.

Dr. Widrow is a past president and member of the Governing Board of the International Neural Network Society. He is associate editor of several journals and is the author of over 125 technical papers and 21 patents. He is co-author of *Adaptive Signal Processing and Adaptive Inverse Control*, both Prentice-Hall books. A new book, *Quantization Noise*, was published by Cambridge University Press in June 2008.



Gregory T. A. Kovacs (M'82-SM'06-F'09) received a BAsC degree in electrical engineering from the University of British Columbia, an MS degree in bioengineering from the University of California, Berkeley, and a PhD in electrical engineering and an MD degree from Stanford University.

He is Director of the Microelectronics Technology Office at DARPA while on leave from Stanford where he is a Professor of Electrical Engineering at Stanford University with a courtesy appointment in the Department of Medicine. He is a long-standing member of the Defense Sciences Research Council (DARPA), and has served as Associate Chair and Chairman. He also has extensive industry experience including co-founding several companies, including Cepheid in Sunnyvale, CA. His present research areas include biomedical instruments and sensors, cardiac physiology, in vitro models for stem cell tissue repair, and medical diagnostics.

In 2003, he served as the Investigation Scientist for the debris team of the Columbia Accident Investigation Board, having worked for the first four months after the accident at the Kennedy Space Center, Florida. He later served as Engineering/Medical Liaison on the Spacecraft Crew Survival Integration Investigation Team (SCSIIT) of the Johnson Space Center. Prof. Kovacs received an NSF Young Investigator Award, held the Noyce Family Chair, and was a Terman and then University Fellow at Stanford. He was the Thomas V. Jones Development Scholar in the School of Engineering from 2003 - 2005. Kovacs is a Fellow of the American Institute for Medical and Biological Engineering and of the IEEE. He is a private pilot, scuba diver, and a Fellow National of the Explorers Club. He was a member of a NASA and National Geographic Society sponsored team that climbed Licancabur volcano (19,734 ft.) on the Chile/Bolivia border in November of 2003, serving as medical, physiologic research, and photography lead. In November of 2004, he served the same role on a return expedition to Licancabur, and carried out medical research and underwater videography in the summit lake.